

# IDENTIFICATION OF MECHANICAL FRACTURE PARAMETERS OF ALKALI-ACTIVATED SLAG BASED COMPOSITES DURING SPECIMENS AGEING

Hana ŠIMONOVÁ<sup>1</sup>, Barbara KUCHARCZYKOVÁ<sup>1</sup>, Martin LIPOWCZAN<sup>1</sup>, David LEHKÝ<sup>1</sup>,  
Vlastimil BÍLEK, Jr.<sup>1,2</sup>, Dalibor KOCÁB<sup>1</sup>

<sup>1</sup>Brno University of Technology, Faculty of Civil Engineering, Veveří 331/95, 602 00 Brno, Czech Republic

<sup>2</sup>Brno University of Technology, Faculty of Chemistry, Purkyňova 464/118, 602 00 Brno, Czech Republic

[simonova.h@vutbr.cz](mailto:simonova.h@vutbr.cz), [barbara.kucharczykova@vutbr.cz](mailto:barbara.kucharczykova@vutbr.cz), [lipowczan.m@fce.vutbr.cz](mailto:lipowczan.m@fce.vutbr.cz), [lehky.d@fce.vutbr.cz](mailto:lehky.d@fce.vutbr.cz),  
[bilek@fch.vut.cz](mailto:bilek@fch.vut.cz), [dalibor.kocab@vutbr.cz](mailto:dalibor.kocab@vutbr.cz)

DOI: 10.35181/tces-2019-0021

**Abstract.** *The aim of the paper is to present the results of the experiment focused on the development of the mechanical fracture characteristics of alkali-activated slag (AAS) based composites within the time interval from 3 days to 2 years of ageing. Two AAS composites, which differed only in the presence of shrinkage reducing admixture (SRA), were prepared for the purpose of experiments. The composites were prepared using ground granulated blast furnace slag activated by water-glass with silicate modulus of 2.0, standardized quartzite sand with the particle grain size distribution of 0–2 mm, and water. Commercially produced SRA was added into the second mixture in an amount of 2 % by weight of slag. The test specimens were not protected from drying during the whole time interval and were stored in the laboratory at an ambient temperature of  $21 \pm 2$  °C and relative humidity of  $60 \pm 10$  %. The prism specimens made of the above-mentioned composites with nominal dimensions of  $40 \times 40 \times 160$  mm with the initial central edge notch were subjected to the fracture tests in a three-point bending configuration. The load  $F$  and displacement  $d$  (deflection in the middle of the span length) were continuously recorded during the fracture tests. The obtained  $F$ – $d$  diagrams and specimen dimensions were used as input data for identification of parameters via the inverse analysis based on the artificial neural network, which aim is to transfer the fracture test response data to the desired material parameters. In this paper, the modulus of elasticity, tensile strength, and fracture energy values were identified and subsequently compared with values obtained based on the fracture test evaluation using the effective crack model and work-of-fracture method.*

## Keywords

**Fracture test, Inverse analysis, Artificial neural network, Effective crack model, Work-of-fracture method, Slag, Alkali activation.**

## 1. Introduction

During recent decades, the research of various non-traditional binders as the modern alternatives to Portland cement has attracted great scientific attention. One wide group of these binders are alkali-activated materials (AAMs) whose setting and hardening processes are based on the dissolution of suitable amorphous aluminosilicate precursors in alkaline solution and condensation of the dissolved species into solid products, typically calcium/sodium-aluminate-silicate-hydrates, whose composition and properties strongly depend on the chemistry of both the precursor and the alkaline activator and as well as on curing conditions [1]. Alkali-activated slag (AAS) usually reaches high mechanical properties even at room temperature, but suffers from extensive shrinkage and cracking, particularly when subjected to drying, which has a negative impact on durability, mechanical parameters, etc.

Acquaintance with the mechanical and especially fracture parameters of composites with a brittle matrix among which also belong AAS is indispensable for the quantification of their resistance to crack initiation and growth, as well as for the specification of material model parameters employed for the simulation of the quasi-brittle behaviour of structures or their parts made from this type of composite. Unfortunately, the literature on the fracture properties of AAS which can be used as suitable inputs for material models is still fairly limited. The most of the currently published articles are only concerned with the determination of basic mechanical parameters, i.e. compressive and flexural strengths, or in some cases modulus of elasticity [2–5].

Therefore, the main attention of this paper is focused on the performing and evaluation of three-point bending fracture tests of prism specimens with an initial central edge notch made of selected AAS based composites.

The attention is also paid to the identification of mechanical fracture parameters based on the evaluation of fracture test records via inverse analysis based on the artificial neural network. The obtained parameters can be used to quantify the structural resistance of the material to the crack initiation and propagation, as well as for the comparison of the studied or developed composites based on the alkali-activated matrix. They can also be employed for the definition of the material models for deterministic or stochastic simulation of the quasi-brittle/ductile response of composite materials using the Stochastic Finite Element Method model with nonlinear fracture mechanics principles implemented, including material uncertainties required for reliability analysis. In this paper, the modulus of elasticity, tensile strength, and fracture energy values were identified and subsequently compared with the values obtained based on the fracture test evaluation using the effective crack model and work-of-fracture method.

## 2. Experimental Investigation

### 2.1. Mixtures and Specimens

AAS based specimens were prepared from ground granulated blast furnace slag, activating solution (water glass + water) and standardized CEN siliceous sand with the grain size of 0–2 mm. Slag contained 90 % of the amorphous phase as determined using X-Ray diffraction and had Blaine fineness of 400 m<sup>2</sup>/kg. Water-glass with Na<sub>2</sub>O content of 17.1% and silicate modulus of 2.0 was used for slag activation at the dose corresponding to 10 % Na<sub>2</sub>O with respect to the slag weight. Water to slag ratio including water from water glass was 0.42 and sand to slag ratio was 3 : 1.

Two sets of test specimens with nominal dimensions of 40 × 40 × 160 mm were prepared for the purpose of fracture tests. The difference between mixtures was only in the presence of shrinkage-reducing admixture (SRA). The sets of specimens were labelled as follows: VIII and IX, specimens without and with SRA, respectively. The commercially available SRA (Stachement AC600) was used and its dose corresponded to 2% of the slag weight. The AAS composites were mixed by a laboratory mixer with a mixing speed of 30 revolutions per minute and then were cast into the polypropylene moulds (see Fig. 1). After 72 hours, specimens were demoulded and stored until the start of experiments. Curing conditions (ambient temperature of 21 ± 2 °C and relative humidity of 60 ± 10 %) were the same before and after demoulding. Such severe curing conditions were selected to intensify shrinkage and to evaluate the effect of the used SRA. In total, 24 specimens were made from each mixture intended for fracture tests; six specimens were tested at each investigated age of specimens. The fracture parameters were determined at the age of 3, 28, 90 days and 2 years.



Fig. 1: Test specimens cast into the polypropylene moulds.

### 2.2. Fracture Tests

The fracture characteristics were determined based on the load  $F$  versus displacement  $d$  (deflection in the middle of the span length) diagrams recorded during the three-point bending test of the prism specimens with an initial notch. The depth of the notch was, in this case, approx. 1/3 of the specimens' height. The span length was set to 120 mm. The specimens were subjected to the quasi-static loading using the mechanical testing machine Heckert FP 10/1 with a constant displacement increment of 0.02 mm/min (see Fig. 2).



Fig. 2: Illustration of performed fracture test.

## 3. Determination of Mechanical Fracture Parameters

### 3.1. Identification

The artificial neural network(ANN)-based inverse analysis method was employed to identify selected mechanical fracture parameters from experimental data acquired during three-point bending tests on the above mentioned notched prism specimens. The inverse procedure developed by Novák and Lehký [6] transforms fracture test response data into the desired mechanical fracture parameters. This approach is based on matching laboratory measurements with the results gained by reproducing the same test numerically. The ANN is used here as a surrogate model of an unknown inverse function between input mechanical fracture parameters and corresponding response parameters.

The set for training the ANN is prepared numerically via the utilization of a finite element method (FEM) model which simulates a three-point bending test with random realizations of material parameters. These are generated using the stratified sampling method and by performing an inverse transformation of the distribution function in order to reflect the probability distribution of the parameter. Conveniently, the ATENA FEM program (Červenka et al. [7]) was employed for the numerical simulation of the fracture test. The 3D NonLinear Cementitious 2 material model was selected to govern the gradual evolution of localized damage.

The utilized identification system consists of an ensemble of neural networks. A three-dimensional space defined by three mechanical fracture parameters – modulus of elasticity  $E_{ID}$ , tensile strength  $f_{t, ID}$ , and specific fracture energy  $G_{F, ID}$  – is divided into several subspaces. Every subspace contains a single robust ANN trained for a limited range of parameters. A suitable subspace for the analysed specimen is automatically selected and the corresponding ANN is activated based on an initial analysis of the experimental response data. The set of mechanical fracture parameters is calculated by simulating the ANN with obtained response parameters. When a specimen has material parameters that are situated close to the boundaries of a subspace and thus may belong to several overlapping subspaces, the final set of parameters is obtained via the weighted averaging of sets of parameters identified by the individual ANNs. For more details on ANN-based identification and utilization of ANN ensemble see [8, 9].

In order to verify the identified material parameters, a numerical FEM analysis is carried out and the resulting numerical  $F-d$  diagrams are compared with the experimental diagrams. See such comparison for the selected specimen from both sets VIII and IX, respectively, tested in 3, 90 days and 2 years in Figs. 3 and 4.

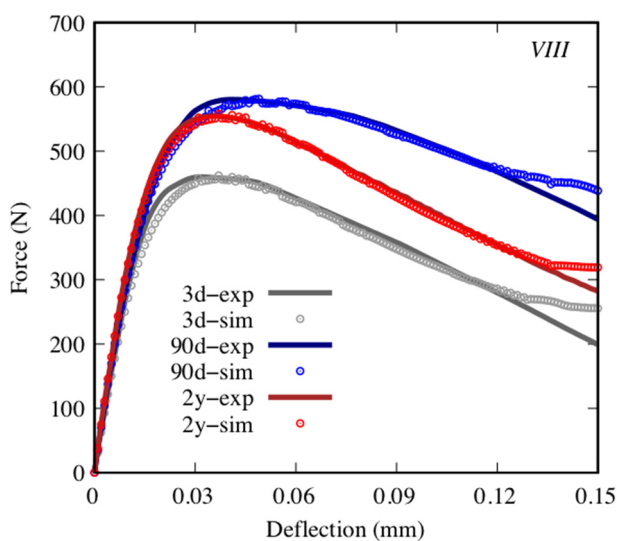


**Fig. 3:** A comparison of experimental and simulated  $F-d$  diagrams: selected specimens from VIII set tested in 3, 90 days and 2 years.

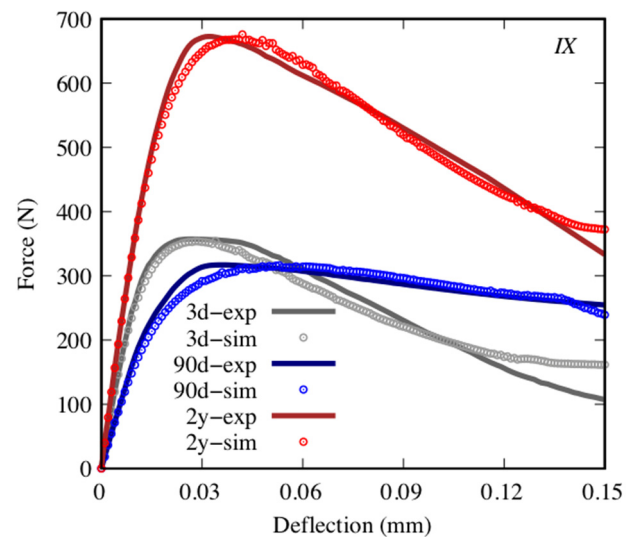


**Fig. 4:** A comparison of experimental and simulated  $F-d$  diagrams: selected specimens from IX set tested in 3, 90 days and 2 years.

### 3.2. Effective Crack Length Method, Work-of-Fracture Method

After the appropriate processing of measured diagrams, at first the ascending parts of  $F-d$  diagrams were used to estimate the modulus of elasticity values according to [10]:

$$E_c = \frac{F_i}{4Bd_i} \left(\frac{S}{D}\right)^3 \left[1 + \frac{5qS}{8F_i} + \left(\frac{D}{S}\right)^2 \left\{2.70 + 1.35 \frac{qS}{F_i}\right\} - 0.84 \left(\frac{D}{S}\right)^3\right] + \frac{9}{2} \frac{F_i}{Bd_i} \left(1 + \frac{qS}{2F_i}\right) \left(\frac{S}{D}\right)^2 F_1(\alpha_0) \quad (1)$$

where  $F_i$  is the load in the initial linear part of the diagram,  $d_i$  is the midspan deflection corresponding to the load level  $F_i$ ,  $B$  and  $D$  are the breadth and depth of the specimen, respectively,  $S$  is the span length,  $q$  is the self-weight of the specimen per unit length and

$$F_1(\alpha_0) = \int_0^{\alpha_0} xY^2(x)dx \quad (2)$$

with  $\alpha_0 = a_0/D$  ( $a_0$  is the depth of the initial notch), and  $Y(x)$  is the geometry function for the three-point bending configuration [10].

After that, the effective fracture toughness  $K_{Icc}$  was determined based on the  $F-d$  diagrams using the effective crack model [10]. The effective crack length  $a_e$  corresponding with the maximum load  $F_{max}$  and matching the midspan deflection  $d_{F_{max}}$ , had to be calculated first. It follows the concept of the effective crack model that the  $a_e$  can be calculated from the equation (1) using  $F_{max}$  and  $d_{F_{max}}$  instead of  $F_i$  and  $d_i$ .

Subsequently, the  $K_{Icc}$  was calculated using the linear elastic fracture mechanics formula according to [10]:

$$K_{Icc} = \frac{3F_{max}S}{2BD^2} Y(\alpha_e) \sqrt{a_e} \quad (3)$$

where  $Y(\alpha_e)$  is the geometry function for the three-point bending configuration [10] and  $\alpha_e = a_e/D$ .

The complete  $F-d$  diagrams, including their post-peak parts, were employed to determine the work of fracture

$W_F^*$  value, which is given by the area under the  $F-d$  diagram. After that, the specific fracture energy  $G_F^*$  values were determined according to the RILEM method [11]:

$$G_F^* = \frac{W_F^*}{B(D-a_0)} \quad (4)$$

The informative compressive strength was determined according to ČSN EN 196-1 [12] on the fragments of the prism specimens obtained after the fracture tests were finished.

## 4. Results

The mean values and coefficient of variations (CoV) of the mechanical fracture parameters after identification of both sets of specimens at the age of 3, 90 days and 2 years are presented in Tab. 1 and 2: modulus of elasticity  $E_{ID}$ , fracture energy  $G_{F, ID}$  and tensile strength  $f_{t, ID}$ . Note that a total of 6 ANNs were employed for the identification of 36 specimens.

**Tab.1:** Mean values (CoV in %) of selected mechanical fracture parameters obtained by identification – set VIII.

Set VIII		Age of specimens		
Parameter	Unit	3 days	90 days	2 years
$E_{ID}$	GPa	14.4 (13.9)	16.8 (5.5)	18.0 (4.9)
$G_{F, ID}$	J/m <sup>2</sup>	140.3 (24.4)	241.5 (29.6)	147.3 (16.5)
$f_{t, ID}$	MPa	1.5 (9.6)	1.7 (10.2)	1.8 (4.3)

**Tab.2:** Mean values (CoV in %) of selected mechanical fracture parameters obtained by identification – set IX.

Set IX		Age of specimens		
Parameter	Unit	3 days	90 days	2 years
$E_{ID}$	GPa	14.4 (14.1)	8.1 (4.6)	19.0 (6.7)
$G_{F, ID}$	J/m <sup>2</sup>	82.3 (21.6)	178.1 (25.8)	204.8 (10.2)
$f_{t, ID}$	MPa	1.2 (7.1)	0.7 (12.2)	2.3 (6.0)

The results of performed direct evaluation of fracture test records using the effective crack model and work-of-fracture method are displayed in Fig. 5 – Fig. 7. The average values accompanied by the sample standard deviations (in form of error bars) are shown for all investigated characteristics. All investigated mechanical fracture parameters showed an unanticipated decrease in their values at the age of 28 days. In the case of specimens without SRA (set VIII), the values decreased to less than 10% of the values determined at the age of 3 days. In the case of specimens with SRA (set IX), the decrease is not such a significant – the values decrease to 25–40% of the values determined at the age of 3 days. Because of this unanticipated decrease, it was decided to exclude this specimen's age from parameter identification.

At the age of 90 days and 2 years, the values of mechanical fracture parameters increased. In general, in the case of set VIII, the values at the age of 90 days are higher in comparison with the values at the age of 3 days. The values at the age of 2 years are similar (when we take into account the standard deviation) for modulus of elasticity and effective fracture toughness in comparison with the values at the age of 90 days. The specific fracture energy values decreased by about 30% in comparison with values obtained at the age of 90 days. On the contrary, in the case of set IX, the values of modulus of elasticity and fracture toughness at the age of 90 days are still lower in comparison with the values at age of 3 days. Nevertheless, the values gradually increase with the specimen's age and at the age of 2 years are comparable or even higher than the values for set VIII.

If the results obtained for the specimens at the age of 28 days are excluded from the evaluation, the same trend of development of modulus of elasticity and fracture energy values is obtained using the parameter identification and direct evaluation for both sets of specimens. When the absolute values are compared, the modulus of elasticity value is by about 20% higher in the case of parameter identification for both sets of specimens. In the case of fracture energy, the difference is higher about 50–75% and 60–90% for set VIII and IX, respectively.

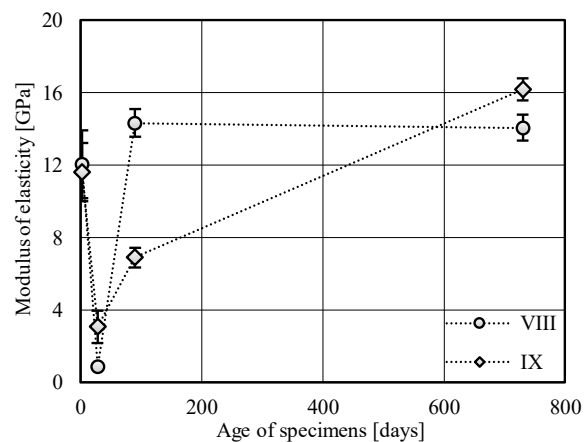


**Fig. 5:** The modulus of elasticity for both AAS composites.

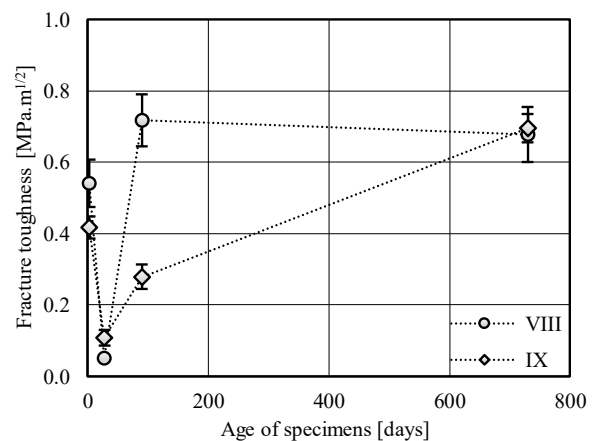


**Fig. 6:** The effective fracture toughness for both AAS composites.



In contrast to the development of the fracture parameters values, the compressive strength values of both sets of specimens noticeably increased between the 3<sup>rd</sup> and 90<sup>th</sup> days of ageing (see Fig. 8). Such different evolution of mechanical properties can be explained by the existence of microcracks to which the fracture test and related fracture parameters are more sensitive in contrast to the common compressive strength test.

The visual inspection was performed before each fracture testing. The gradual development of the shrinkage cracks on the specimens' surface was observed between the age of 3 and 28 days when the cracks were most visible. No cracks were observed on the specimens' surface at the age of 90 days and 2 years. Hypothetically, the relative humidity of about 60% was low enough to induce early age cracking of AAS specimens but simultaneously high enough to allow slow hydration resulting in a certain self-healing process. Nevertheless, further investigation has to be performed.

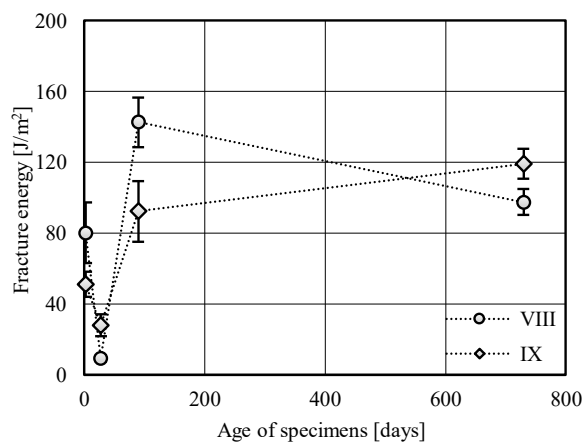


Fig. 7: The specific fracture energy for both AAS composites.

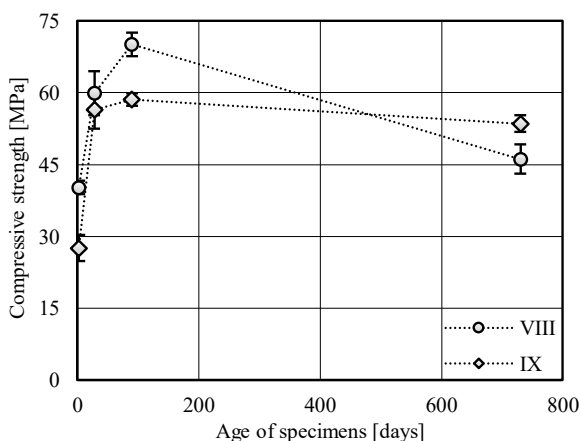


Fig. 8: The informative compressive strength for both AAS composites.

## 5. Conclusions

Fracture tests and the subsequent evaluation of the mechanical fracture parameters of specimens made of

fine-grained composite based on alkali-activated slag was described. Determination of the parameters was performed using two techniques – inverse analysis using an artificial neural network-based method and the direct evaluation of parameters from an experimentally obtained  $F-d$  diagrams by the effective crack model and work-of-fracture method. The results of both evaluation approaches were compared; both techniques provided comparable results (similar trend of parameter development during the ageing). The differences in mean values of fracture energy correspond to their different physical meanings – the identified values are primarily related to the material point, whereas the values obtained from the work-of-fracture method are related to the tested specimen, the size, and shape of fracture process zone and represent the average fracture energy. The significant advantage is that the inverse analysis additionally provides values for the tensile strength of the tested composite. The  $F-d$  diagrams obtained from numerical simulations of specimens with identified parameters show very good agreement with those derived from experiments. The results can serve efficiently as input data for the stochastic nonlinear simulation of the studied material

The effect of the shrinkage-reducing admixture on the values of mechanical fracture parameters was also studied. The addition of SRA had in this particular case a negative effect on the development of mechanical fracture parameters within the time interval from 3 days to 90 days of ageing when the values of all monitored parameters were lower in comparison with specimens without SRA. An exception was the results obtained at the age of 28 days when the monitored mechanical fracture parameters were slightly higher in the case of AAS composite with SRA. However, it should be noted that unanticipated decrease in all investigated parameters was observed for both tested AAS composites at the age of 28 days. Further investigation has to be performed to find out its origin. From the point of view of long term properties (at the age of 2 years), the AAS composite with SRA shows higher values of all monitored parameters in comparison to the AAS composite without SRA.

## Acknowledgements

This outcome has been achieved with the financial support of the Czech Science Foundation under project No 18-12289Y and the specific university research project granted by the Brno University of Technology, registered under the number FAST- J-19-6040.

## References

- [1] PROVIS, J. L. and VAN DEVENTER, J. S. J. (eds.). *Alkali Activated Materials: State-of-the-Art Report*, RILEM TC 224-AAM. Dordrecht: Springer 2014. ISBN 978-94-007-7671-5.

- [2] MARJANOVIĆ, N., M. KOMLJENOVIĆ, Z. BAŠČAREVIĆ, V. NIKOLIĆ and R. PETROVIĆ. Physical–mechanical and microstructural properties of alkali-activated fly ash–blast furnace slag blends. *Ceramics International*. 2015, vol. 41, iss. 1, pp. 1421–1435. ISSN 0272-8842. DOI: <https://doi.org/10.1016/j.ceramint.2014.09.075>
- [3] AYIDIN, S. and B. BARADAN. Effect of activator type and content on properties of alkali-activated slag mortars. *Composites part B: Engineering*. 2014, vol. 57, pp. 166–172. ISSN 1359-8368. DOI: <https://doi.org/10.1016/j.compositesb.2013.10.001>
- [4] RASHAD, A. M. A comprehensive overview about the influence of different additives on the properties of alkali-activated slag – A guide for Civil Engineer. *Construction and Building Materials*. 2013, vol. 47, pp. 29–55. ISSN 0950-0618. DOI: <https://doi.org/10.1016/j.conbuildmat.2013.04.011>
- [5] PUERTAS, F., T. AMAT, A. FERNÁNDEZ-JIMÉNEZ and T. VÁZQUEZ. Mechanical and durable behaviour of alkaline cement mortars reinforced with polypropylene fibres. *Cement and Concrete Research*. 2003, vol. 33, pp. 2031–2036. ISSN 0008-8846. DOI: [https://doi.org/10.1016/S0008-8846\(03\)00222-9](https://doi.org/10.1016/S0008-8846(03)00222-9)
- [6] NOVÁK, D. and D. LEHKÝ. ANN Inverse Analysis Based on Stochastic Small-Sample Training Set Simulation. *Engineering Application of Artificial Intelligence*. 2006, vol. 19, pp. 731–740. ISSN 0952-1974. DOI: <https://doi.org/10.1016/j.engappai.2006.05.003>
- [7] ČERVENKA, V., L. JENDELE and J. ČERVENKA. ATENA program documentation – Part 1: theory. Prague: Cervenka Consulting Ltd., 2016.
- [8] LEHKÝ, D., Z. KERŠNER and D. NOVÁK. FraMePID-3PB Software for Material Parameters Identification Using Fracture Test and Inverse Analysis. *Advances in Engineering Software*. 2014, vol. 72, pp. 147–154. ISSN 0965-9978. DOI: <https://doi.org/10.1016/j.advengsoft.2013.10.001>
- [9] LEHKÝ, D., M. LIPOWCZAN, H. ŠIMONOVÁ and Z. KERŠNER. A neural network ensemble for the identification of mechanical fracture parameters of fine-grained brittle matrix composites. In: *10<sup>th</sup> International Conference on Fracture Mechanics of Concrete and Concrete Structures (FraMCoS-X)*, Bayonne, France: 2019 (in print).
- [10] KARIHALOO, B. L. *Fracture Mechanics and Structural Concrete*. New York: Longman Scientific & Technical 1995. ISBN 978-0582215825
- [11] RILEM TC – 50 FMC (Recommendation): Determination of the fracture energy of mortar and concrete by means of three-point bend test on notched beams. *Materials and Structures*. 1985, vol. 18, iss. 4, pp. 287–290. ISSN 1359-5997. DOI: <https://doi.org/10.1007/BF02472918>
- [12] ČSN EN 196-1 *Methods of testing cement – Part 1: Determination of strength*. Prague: ÚNMZ, 2016.

## About Authors

**Hana ŠIMONOVÁ** was born in Slaný, Czech Republic. She received her B.Sc., M.Sc., and Ph.D. degrees in Civil Engineering from the Brno University of Technology, Faculty of Civil Engineering (BUT), Czech Republic in 2008, 2010 and 2013, respectively. Her current research interests include fatigue and fracture mechanics of quasi-brittle composites field, evaluation of fatigue and static fracture tests of many different types of materials based on the brittle matrix.

**Barbara KUCHARCZYKOVÁ** was born in Trinec, Czech Republic. She received the M.Sc., and Ph.D. degrees in Civil Engineering from the Brno University of Technology (BUT), Czech Republic in 2003 and 2008, respectively. Her current research interests include the technology of production of cement composites, design and implementation of experimental analysis and testing methods used for measurement and evaluation of the characteristics of building materials.

**Martin LIPOWCZAN** was born in Frýdek-Místek, Czech Republic. He received his B.Sc., and M.Sc. degrees in Civil Engineering from Brno University of Technology, Faculty of Civil Engineering (BUT), Czech Republic in 2014 and 2018, respectively. His research interests include identification of mechanical fracture parameters, fracture mechanics and utilization of soft computing methods in structural engineering.

**David LEHKÝ** was born in Moravský Krumlov, Czech Republic. He received his M.Sc., Ph.D., and Assoc. Prof. degrees in Civil and Structural Engineering from Brno University of Technology, Faculty of Civil Engineering (BUT), Czech Republic in 2000, 2006 and 2017, respectively. His research interests include structural safety and reliability, fracture mechanics, identification of material parameters, reliability-based optimization, and utilization of soft computing methods in structural engineering.

**Vlastimil BÍLEK, jr.** was born in Vyškov, Czech Republic. He received his B.Sc., M.Sc., and Ph.D. degrees from BUT (Faculty of Chemistry) in 2011, 2013 and 2017, respectively. His research interests include research and development of non-traditional binders, particularly alkali-activated materials, monitoring their hydration and the application of both organic and inorganic additives to these systems.

**Dalibor KOCÁB** was born in Brno, Czech Republic. He received the M.Sc., and Ph.D. degrees in Civil Engineering from the Brno University of Technology (BUT) in 2008 and 2016, respectively. His main area of research focuses on non-destructive testing, particularly on the ultrasonic pulse velocity test and resonance method.